

# Effect of Flow History on Poly(vinylidene fluoride) Crystalline Phase Transformation

Hadi Sobhani, Mohammad Razavi-Nouri, Ali Akbar Yousefi

Department of Plastics, Faculty of Processing, Iran Polymer and Petrochemical Institute, P.O. Box 14965/115, Tehran, Iran

Received 3 June 2006; accepted 31 July 2006

DOI 10.1002/app.25519

Published online 3 January 2007 in Wiley InterScience (www.interscience.wiley.com).

**ABSTRACT:** This study was devoted to the effect of extensional flow during film extrusion on the formation of the  $\beta$ -crystalline phase and on the piezoelectric properties of the extruded poly(vinylidene fluoride) (PVDF) films after cold drawing. The PVDF films were extruded at different draw ratios with two different dies, a conventional slit die and a two-channel die, of which the latter was capable of applying high extensional flow to the PVDF melt. The PVDF films prepared with the two-channel die were drawn at different temperatures, strain rates, and strains. The optimum stretching conditions for the achievement of the maximum  $\beta$ -phase content were determined as follows: temperature = 90°C, strain = 500%, and strain rate = 0.083 s<sup>-1</sup>. The samples pre-

pared from the dies were then drawn under optimum stretching conditions, and their  $\beta$ -phase content and piezoelectric strain coefficient ( $d_{33}$ ) values were compared at equal draw ratios. Measured by the Fourier transform infrared technique, a maximum of 82%  $\beta$ -phase content was obtained for the samples prepared with the two-channel die, which was 7% higher than that of the samples prepared by the slit die. The  $d_{33}$  value of the two-channel die was 35 pC/N, which was also 5 pC/N higher than that of the samples prepared with the slit die. © 2007 Wiley Periodicals, Inc. *J Appl Polym Sci* 104: 89–94, 2007

**Key words:** crystal structures; extrusion; drawing

## INTRODUCTION

Within the last 2 decades, poly(vinylidene fluoride) (PVDF) has been extensively studied. This is because of the extraordinary pyroelectric and piezoelectric properties that PVDF can present by its microscopic polarization.<sup>1,2</sup> PVDF is a semicrystalline polymer in which five crystallographic forms are observed with different conformations that is, TG<sup>+</sup>TG<sup>-</sup> in the  $\alpha$  and  $\delta$  phases, all-trans (TTT) planar zigzag in the  $\beta$  phase, and T<sub>3</sub>G<sup>-</sup>T<sub>3</sub>G<sup>+</sup> in the  $\gamma$  and  $\epsilon$  phases.<sup>3–5</sup> These crystalline forms can transform to each other under specific conditions, such as under the application of mechanical deformation and a high-temperature electrical field.<sup>6–8</sup> The  $\alpha$ -crystalline form does not show a net lattice polarization due to the antiparallel TG<sup>+</sup>TG<sup>-</sup> chain arrangement in its unit cell. Therefore, the chain dipoles oppose each other. The  $\beta$  form consists of parallel packing of the polymer chains in all-trans conformations, and thus, it shows a large spontaneous lattice polarization.<sup>9–11</sup> The polar  $\beta$  phase is the most desirable crystalline form for PVDF because it provides better pyroelectric and piezoelectric properties. Although the most common polymorph of PVDF is the  $\alpha$  form, which is directly produced by the cooling of the melt, PVDF films

consisting of  $\beta$  crystals are usually prepared by the drawing of samples having  $\alpha$  crystals at temperatures below 100°C and stretching ratios of 3–5.<sup>3,12–14</sup>

A two-channel flow geometry having converging walls was already modeled by Khomami and McHugh.<sup>15,16</sup> This is a geometry consisting of two flow channels approaching at an angle of  $\gamma$  to form a single converging-wall downstream channel with a converging angle of  $\alpha$ . Their calculations showed that in this geometry, a strong extensional flow existed in the stream impingement region, which remained throughout the converging channel region, and the extensional flow increased with increasing  $\gamma$  angle. With their results, a die was designed by Solid Work Software and was then constructed.<sup>17</sup> Figure 1 shows a schematic of the designed die, which consists of a straight channel entrance section followed by a bifurcation insert in which the split streams were made to impinge at a  $\gamma$  angle of 70° followed by a downstream converging flow with a  $\alpha$  angle of 15°.

In this study, we aimed to explore the effect of extensional flow during film extrusion on the  $\beta$  phase content and on the piezoelectric properties of PVDF films after cold drawing. The PVDF films were extruded at different draw ratios with slit<sup>18</sup> and two-channel dies. The films were then drawn at different temperatures, strain rates, and strains, and the effects of different conditions on the formation of the  $\beta$  phase were investigated. The optimum stretching conditions were determined to achieve to the

Correspondence to: A. A. Yousefi (a.yousefi@ippi.ac.ir).

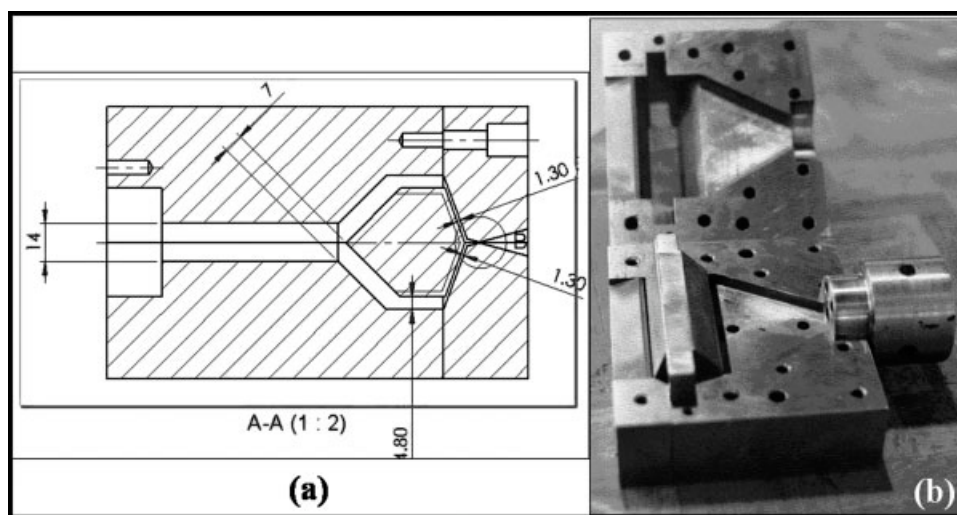


**Figure 1** Two-channel die: (a) sketch of the die dimensions (in millimeters) and (b) photograph of the die.

highest  $\beta$ -phase content. Finally, the samples prepared from both dies were drawn under optimum conditions, and their  $\beta$ -phase contents and the piezoelectric strain coefficient ( $d_{33}$ ) values were compared at equal draw ratios.

## EXPERIMENTAL

### Material

PVDF was supplied by Ausimont, Inc. (New Jersey, USA), and was grade Hylar 460. The weight-average molecular weight was 236 kg/mol, and the melting point was 160°C.

### Film extrusion

The PVDF films were prepared by extrusion through a single-screw extruder. The extruder was a laboratory extruder (Haake HBI Sys 90; Karlsruhe, Germany) equipped with a screw 0.02 m in diameter with a length/diameter ratio of 24 : 1 and a compression ratio of 3/1 (the initial height of the screw channel was three times greater than the final height). During extrusion, the temperature was set to 220°C at the feeding zone and increased to 240°C at the die. Two different dies were used to produce the films, that is, a slit die and a two-channel die. Both dies had the same split die gauge of 250  $\mu\text{m}$ . Three steel rolls, each 0.0764 m in diameter, were used to take up the films. By adjusting the speed of rotating rolls, we were able to control the melt draw ratio and also the thickness of the PVDF films. The take-up speed was variable in the range 1.48 to 13.32 rpm. The extrusion speed (the speed of the melt just after it exited the die) was measured to be 0.006 m/s, and thus, the melt draw ratio was in the range 1–9.

### Cold drawing

For uniaxial stretching, the films were mounted on the stretching device in an air circulating oven and drawn at different temperatures, strain rates, and strains. Before extension, the samples rested in the oven at the stretching temperature for 10 min to equilibrate at the test temperature. The heater was turned off after the stretching process, and the drawn samples were slowly cooled in the oven for the next 20 min. The original width and gauge length of the films were 0.03 and 0.1 m, respectively. The different stretching conditions used to determine the optimum cold drawing conditions are summarized in Table I.

### Polarization

Poling of the samples was carried out in an electrical field of 125 MV/m at 80°C. The  $d_{33}$  values of the polarized films were then measured with a  $d_{33}$  meter (APC Int., Ltd., model 8000; Pennsylvania, USA). The  $d_{33}$  meter was used at an operating frequency of 1000 Hz and with a time interval of 24 h after polarization of the films.

### Fourier transform infrared (FTIR) spectroscopy

Identification of the crystalline phases present in each sample was performed by means of an FTIR spectrometer (Bruker, model IFS48; Ettlingen, Germany) in the wave-number range 400–1000  $\text{cm}^{-1}$ . The vibration bands at wave numbers of 614, 765, and 975  $\text{cm}^{-1}$  represented the  $\alpha$  phase, and the vibration band at 840  $\text{cm}^{-1}$  corresponded to the  $\beta$  phase. FTIR accurately measured the variation of the  $\beta$  phase in the polymer films. The fraction of  $\beta$ -phase crystals in each sample was calculated according to the specific absorption bands of the  $\alpha$  and  $\beta$  phases.

TABLE I  
Different Stretching Conditions Applied to the Samples

Temperature = 90°C and strain = 300%					
Strain rate (s <sup>-1</sup> )	0.004	0.025	0.050	0.083	
Temperature = 90°C and strain rate = 0.083 s <sup>-1</sup>					
Strain (%)	100	200	300	400	500
Strain rate = 0.083 s <sup>-1</sup> and strain = 500%					
Temperature (°C)	70	80	90	100	110

On the basis of the Beer–Lambert law, an equation was obtained by Gregorio and Cestari<sup>19</sup> to calculate the  $\beta$ -phase fraction [ $F(\beta)$ ]:

$$F(\beta) = \frac{X_{\beta}}{X_{\alpha} + X_{\beta}} = \frac{A_{\beta}}{1.26A_{\alpha} + A_{\beta}} \quad (1)$$

where  $X_{\alpha}$  and  $X_{\beta}$  are the crystalline mass fractions of the  $\alpha$  and  $\beta$  phases, respectively, and  $A_{\alpha}$  and  $A_{\beta}$  are their absorption bands at 764 and 840 cm<sup>-1</sup>, respectively.

#### Wide-angle X-ray diffraction (WAXD)

The diffraction lines of the samples were obtained with a Philips X-ray diffractometer (Almelo, The Netherlands), which was interfaced to a PC and operated with Cu K $\alpha$  radiation ( $\lambda = 1.54 \text{ \AA}$ ). The scans were recorded at  $2\theta$  values of 10–40° with steps of 0.02°. The counting time was 1 s per step.

#### Mechanical properties

The tensile properties of the films were measured with an Instron model 6025 instrument (High Wycombe, UK). All tests were carried out at a constant temperature of 23°C, a relative humidity of 35%, and an extension rate of  $8.3 \times 10^{-4} \text{ m/s}$  according to ASTM D 882.

### RESULTS AND DISCUSSION

To study the effect of strain rate on  $\beta$ -phase formation, the PVDF film produced by the two-channel die at a maximum possible draw ratio of 9 (ref. 17) was stretched at different strain rates but at constant temperature of 90°C<sup>14,19</sup> and an arbitrary strain of 300%. FTIR spectra of the samples were then prepared, and  $F(\beta)$  of the films was calculated according to eq. (1). The results are shown in Figure 2.  $F(\beta)$  increased with the rate of stretching, and the highest  $\beta$ -phase content was obtained at the highest possible strain rate of 0.083 s<sup>-1</sup>.

The difference between the  $\beta$ -phase content in the samples drawn at low and high strain rates could be explained by the fact that at lower deformation rates, the concentration of local stress on the crystals for the destruction of crystalline order was low. During stretching, amorphous sections were drawn first, and the polymer chains were oriented along the

stretching direction. Then, the applied stress was transferred into the crystals, and crystalline order began to be destroyed. Consequently, stress was rapidly relaxed in the amorphous sections, and the efficiency of stress for the destruction of crystalline order was decreased at low strain rates. The effect of stress relaxation was evident in the  $\alpha$ - to  $\beta$ -phase transformation. Sajkiewicz et al.<sup>6</sup> reported that at low deformation rates, the applied stress during stretching largely relaxes. This leads to a low orientation of crystallites and, thus, to a low  $\alpha$ - to  $\beta$ -phase transformation. As a result, the transformation increases with increasing strain rate.

To investigate the effect of strain on  $\alpha$ - to  $\beta$ -phase transformation, the PVDF films prepared at the initial draw ratio of 9 were drawn to different strains but at a constant temperature of 90°C and a strain rate of 0.083 s<sup>-1</sup>. The FTIR spectra of the films drawn to different strains are shown in Figure 3. According to the characteristic absorption band of the  $\beta$  phase at 840 cm<sup>-1</sup> and those of the  $\alpha$  phase at 614, 765, and 975 cm<sup>-1</sup>, a complete predominance was observed for  $\alpha$ - and  $\beta$ -phase contents for the samples that were drawn to 100 and 500%, respectively.

Figure 4 shows the variation of  $F(\beta)$  with strain.  $F(\beta)$  increased with increasing strain, and the highest  $\beta$ -phase content was obtained when the strain passed 400%. Matsushige et al.<sup>20</sup> suggested that a heterogeneous stress distribution in the sample has a critical role in the crystal transformation phenom-

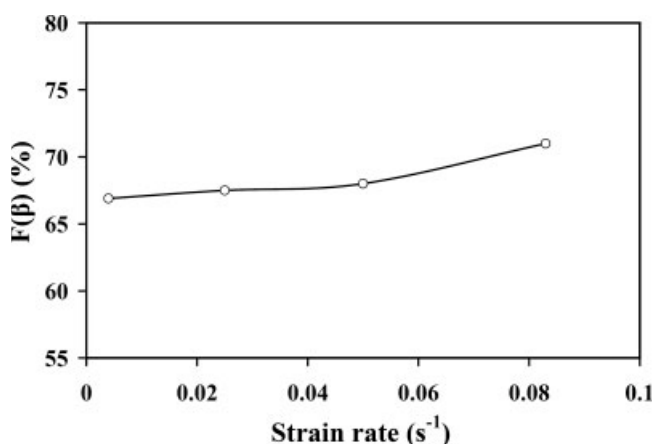
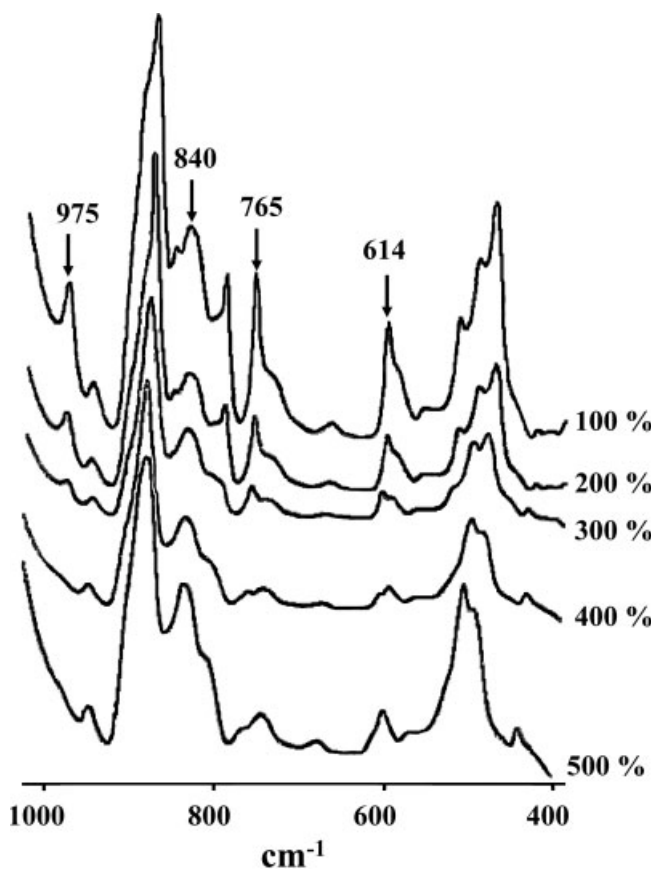


Figure 2 Variation of the  $\beta$ -phase content as a function of strain rate.



**Figure 3** FTIR spectra of the films stretched to different strains.

enon during  $\alpha$ - to  $\beta$ -phase transformation under tensile stress. They found that the transformation occurs at the stage where necking is initiated at the center of the tensiled samples.

During necking, small blocks of lamella are torn away from the original lamella to form crystallites with fibrillar structure. This mechanism induces an all-trans planar zigzag conformation ( $\beta$  phase) into the crystals.<sup>3</sup> During the deformation of PVDF, a critical stress was reached at which rotation around C—C bonds became possible, and not only were the polymer chains oriented in the direction of stretching, but also the segments with an  $\alpha$ -phase structure were transformed into a  $\beta$ -phase crystalline structure. In other segments that were stretched below the critical stress, the original structure remained intact, and therefore, in addition to the well-oriented  $\beta$ -phase crystals, unoriented  $\alpha$ -phase crystals were also found in the neck region.<sup>14,21</sup>

The neck region developed to the end of samples at an extension larger than 200%. Figure 4 shows that the  $\beta$ -phase content increased significantly right after the neck had fully developed. Then, we concluded that the critical stress for converting the  $\alpha$  phase to the  $\beta$  phase was reached whenever the sample was stretched a strain higher than 200%.

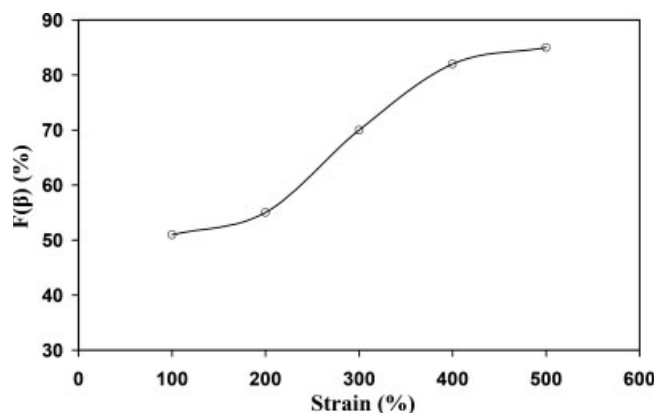


**Figure 4** Variation of the  $\beta$ -phase content against the strain.

The WAXD spectra of the samples drawn to various strains are shown in Figure 5. The diffraction lines of the unstretched films were present at  $2\theta$  values of 17.8, 18.4, and 20°. These lines represented diffractions from the [100], [020], and [110] lattice planes for the  $\alpha$ -crystalline form, respectively. For the stretched films, the peaks appearing at  $2\theta$  values of 17.8 and 18.4° overlapped, and their intensities decreased. However, the diffraction line at  $2\theta = 20^\circ$  shifted to 20.5°, of which the latter represented diffraction from the [110] and [200] lattice planes of the  $\beta$  structure. The diffraction lines related to the  $\alpha$  phase disappeared at strains higher than 200%, and only the diffraction line at  $2\theta = 20.5^\circ$  remained at strains higher than 300%.

To obtain the optimum stretching temperature, the films prepared at an initial draw ratio of 9 were strained to 500% with a strain rate of  $0.083 \text{ s}^{-1}$  at different temperatures. The variation of  $\beta$ -phase content with stretching temperature is shown in Figure 6. The maximum  $\beta$ -phase formation was obtained at a stretching temperature of about 90°C. At temperatures lower than 90°C, the viscosity of the polymer

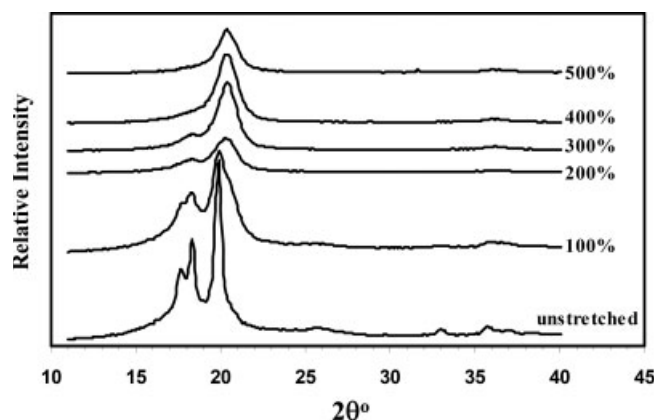


**Figure 5** WAXD spectra of the films stretched to different strains.



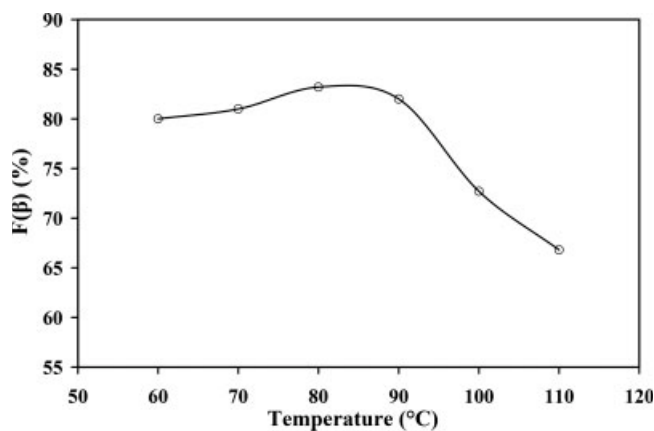


**Figure 6** Variation of the  $\beta$ -phase content against the stretching temperature.

was very high, and the stress, which was induced by deformation, was sufficient to destroy the crystalline order. The crystals were reorganized in the phase that was stable the most at the processing temperature when drawing was ceased. Because the crystallization rate of the  $\beta$  phase in this temperature range was higher than that of the  $\alpha$  phase, reorganization occurred mostly in the form of the  $\beta$  phase.<sup>6</sup>

Therefore, the optimum conditions for cold drawing were achieved at a temperature of about 90°C, a strain of 500%, and a strain rate of 0.083 s<sup>-1</sup>.

The effect of initial draw ratio (during extrusion) on the final  $\beta$ -phase content after cold drawing was also investigated. The PVDF films prepared with different initial draw ratios were drawn at optimum conditions. Figure 7 shows the variation of the  $\beta$ -phase content with draw ratio. The  $\beta$ -phase content increased with drawing ratio, and it remained relatively constant after a draw ratio of 6.

To study the effect of extensional flow during extrusion on the final  $\beta$ -phase content, the films prepared with both dies with initial draw ratios of 7 and 9 were compared with each other. The samples were cold

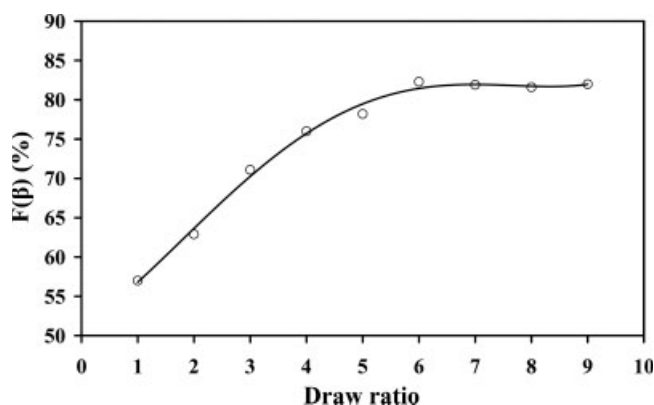


**Figure 7** Variation of the  $\beta$ -phase content as a function of the draw ratio.

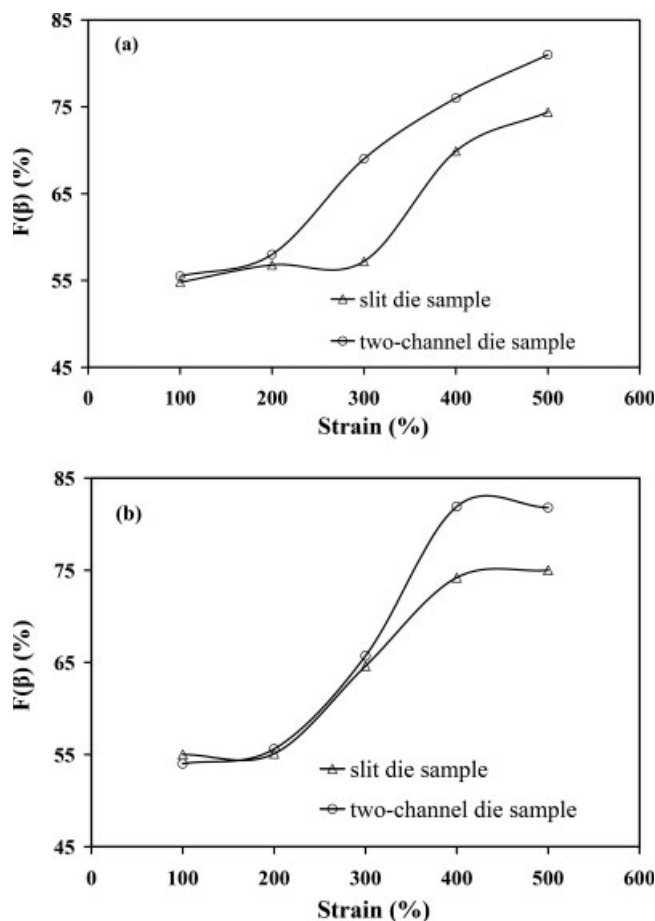


**Figure 8** Variation of the  $\beta$ -phase content against the strain for the films prepared with the two different dies at draw ratios of (a) 7 and (b) 9.

drawn at the optimum temperature and strain rate but to different strains, and their  $\beta$ -phase contents and  $d_{33}$  values were then compared at the same draw ratio. Figure 8(a,b) exhibits the variation of  $F(\beta)$  with strain at two initial draw ratios of 7 and 9, respectively. As shown, at stresses lower than the critical stress that was required to reach 200% strain, the  $\beta$ -phase content in the films prepared by both dies did not change significantly. However,  $F(\beta)$  calculated for the samples prepared with the two-channel die was 82% at a strain of 500%, which was 7% higher than that of the samples prepared with the slit die.

Table II shows the moduli of the films prepared by the two dies at the same draw ratio of 9. The sample

**TABLE II**  
Mechanical Properties of the Films Prepared with the Two Different Dies at a Draw Ratio of 9

Sample	Young's modulus (MPa)	Yield stress (MPa)
Slit die	1350	41
Two-channel die	1480	44

**TABLE III**  
 **$\beta$ -Phase Content and  $d_{33}$  Values After the Cold Drawing of the Films Prepared with the Dies at Two Different Draw Ratios**

Sample	Draw ratio	$\beta$ -phase content (%)	$d_{33}$ (pC/N)
Slit die	7	74	28
	9	75	30
Two-channel die	7	81	34
	9	82	35

prepared with two-channel die had a higher modulus and yield stress than those of the samples prepared with the slit die. These higher mechanical properties were attributed to the existence of elongational flow in the two-channel die, which profoundly increased polymer chain orientation in the flow direction. The applied stress was carried largely by the covalent bonds in the sample with chain orientation.

These results demonstrate that the application of extensional flow to the PVDF melt during extrusion led to chain orientation, and because of rapid cooling of the films under stretching, the induced orientation of amorphous parts between spherulites mostly remained unchanged after declamping. The induced orientation on polymer chains improved the stress efficiency in cold drawing, and it finally increased the formation of the  $\beta$  phase. This was in agreement with results reported by other workers.<sup>7,22</sup>

The piezoelectric properties of the polarized PVDF films significantly depended on the  $\beta$ -phase content.<sup>10,14</sup> The  $d_{33}$  values of the films prepared with both dies after cold drawing to two different draw ratios are reported in Table III. Table III shows that the  $d_{33}$  values of the PVDF films prepared with the two-channel die were higher than those obtained from the sample prepared with the slit die with the same draw ratio. The higher piezoelectric activity of the films prepared with the two-channel die were attributed to the higher chain extension, orientation, and morphological continuity along the film axis and also to the higher  $\beta$ -phase content.

## CONCLUSIONS

The results of cold drawing show that the  $\beta$ -phase content increased with increasing strain and strain rate and reached a maximum value at a certain stretching temperature. The optimum stretching conditions were found at a temperature of around 90°C, a strain of 500%, and a strain rate of 0.083 s<sup>-1</sup>.

Studies on the effect of the initial draw ratio on the final  $\beta$ -phase content after cold drawing also revealed that the  $\beta$ -phase content dramatically increased with draw ratio up to a draw ratio of 6 and then leveled off.

A maximum amount of 82% was measured by the FTIR technique for the  $\beta$ -phase content of the samples prepared with the two-channel die under the optimum stretching conditions. This value was 7% higher than that of the films prepared with the slit die. The  $d_{33}$  value of the samples prepared by the two-channel die was 35 pC/N, which was 5 pC/N higher than that of the samples produced by the slit die.

The improvement of the stress efficiency for the destruction of the crystalline order in the cold-drawing step and also the increase in the  $\beta$ -phase content and, thus,  $d_{33}$  value in the samples prepared with the two-channel die was attributed to the orientation induced by elongational flow to the polymer melt during extrusion.

The authors thank the NEDSA (Neirooye Defa Saheli) Research Center for providing them with polymeric materials and piezoelectric measurement data.

## References

- Masayuki, N.; Nakamura, K.; Uehara, H.; Kanamoto, T.; Takahashi, Y.; Furukawa, T. *J Polym Sci Part B: Polym Phys* 1999, 37, 2549.
- Davis, G. T. *The Applications of Ferroelectric Polymers*; Blackie: London, 1988; Chapter 3.
- Salimi, A.; Yousefi, A. A. *Polym Test* 2003, 22, 696.
- Lovinger, A. J. *Macromolecules* 1982, 15, 40.
- Bendetti, E.; Catanorchi, S.; Dalessio, A.; Moggi, G.; Vergamini, P.; Parcella, M.; Ciardelli, G. *Polym Int* 1996, 41, 35.
- Sajkiewicz, P.; Wasiak, A.; Goclowski, Z. *Eur Polym J* 1999, 35, 423.
- Nakamura, K.; Sawal, D.; Watanabe, Y.; Taguchi, D.; Takahashi, Y.; Furukawa, T.; Kanamoto, T. *J Polym Sci Part B: Polym Phys* 2003, 41, 1701.
- Nakamura, K.; Nagal, M.; Kanamoto, T.; Takahashi, Y.; Furukawa, T. *J Polym Sci Part B: Polym Phys* 2001, 39, 1371.
- Elmohajir, B. E.; Heymans, N. *Polymer* 2001, 42, 5661.
- Gregorio, R.; Cestari, M. *J Mater Sci* 1999, 34, 4489.
- Jungnickel, B. J. *Poly(vinylidene fluoride) (Overview)*; CRC: New York, 1996; p 7115.
- Teyssedre, G.; Bernes, A.; Lacabanne, C. *J Polym Sci Part B: Polym Phys* 1993, 31, 2027.
- Esterly, D. M.; Love, B. J. *J Polym Sci Part B: Polym Phys* 2004, 42, 91.
- Salimi, A.; Yousefi, A. A. *J Polym Sci Part B: Polym Phys* 2004, 42, 3487.
- Khomami, B.; McHugh, A. J. *J Appl Polym Sci* 1987, 33, 1495.
- Khomami, B.; McHugh, A. J. *J Appl Polym Sci* 1988, 36, 859.
- Sobhani, H.; Yousefi, A. A.; Razavi-Nouri, M. *Iran J Polym Sci Tech* 2006, 19, 43 (in Persian).
- Yousefi, A. A.; Salimi, A. Report of Project; Project No. 809j394; Iran Polymer and Petrochemical Institute: Tehran, Iran, 2001.
- Gregorio, R.; Cestari, M. *J Polym Sci Part B: Polym Phys* 1994, 32, 859.
- Matsushige, K.; Nagata, K.; Imada, S.; Takemora, T. *Polymer* 1980, 21, 1391.
- Hsu, T. C.; Geil, P. H. *J Mater Sci* 1989, 24, 1219.
- Khomami, B.; McHugh, A. J. *J Appl Polym Sci* 1988, 36, 877.